



Influence of the calcination treatment on the catalytic properties of hierarchical ZSM-5

D.P. Serrano^{a,b,*}, R.A. García^a, M. Linares^a, B. Gil^c

^a ESCET, Rey Juan Carlos University, c/Tulipán s/n, 28933, Móstoles, Madrid, Spain

^b IMDEA Energy Institute, c/Tulipán s/n, 28933, Móstoles, Madrid, Spain

^c Faculty of Chemistry, Jagiellonian University, Ingardena 3, 30-060 Kraków, Poland

ARTICLE INFO

Article history:

Received 15 April 2011

Received in revised form 15 June 2011

Accepted 17 June 2011

Available online 29 July 2011

Keywords:

Hierarchical ZSM-5 zeolite

Calcination procedure

Friedel–Crafts acylation

Epoxide rearrangement

ABSTRACT

The effect of the calcination conditions on the properties and catalytic performance of hierarchical ZSM-5 zeolite has been investigated using different reactions as catalytic tests: acylation of aromatic substrates and rearrangement of linear and cyclic epoxides. The hierarchical h-ZSM-5 material was prepared by crystallization of silanized protozeolitic units. The removal of the organics present in the as-synthesized ZSM-5 samples has been carried out using two different calcination procedures: (i) directly under air atmosphere; (ii) following a two-step (nitrogen-air) treatment.

Clear differences are noticed related to the textural properties of the ZSM-5 samples, since the h-ZSM-5 presents higher BET and external surface area than standard ZSM-5 zeolite. Whereas the calcination method does not affect the properties of the reference ZSM-5 sample, noticeable changes were observed over the hierarchical zeolite. The concentration of Brønsted acid sites decreases by half for one-step air calcination, but only a quarter when using a two-step nitrogen/air calcination, showing that the aluminium present in hierarchical ZSM-5 is very sensitive to the calcination conditions as it may undergo framework extraction and dehydroxylation phenomena. For all the studied reactions, the hierarchical sample, calcined by a two-step treatment, presents higher activity than when using direct air calcination.

© 2011 Elsevier B.V. All rights reserved.

1. Introduction

Zeolites are crystalline inorganic materials having dimensions in the molecular scale. Zeolites possess singular properties which explain their high interest and potential for being employed in a variety of fields, such as catalysis, ion exchange, separations, adsorption, membranes, optics, etc. Thus, zeolites have found widespread use as heterogeneous catalysts in oil refining, petrochemistry, fine chemistry and pollutant abatement [1].

It is well known that the presence of aluminium in the zeolite framework induces a negative charge that requires a cation to balance it. This is the origin of many zeolite properties, as it is the case of their acidity and capability to catalyze acid reactions. Both Brønsted and Lewis acid sites are typically found in zeolites, their relative proportion depending on the Si/Al ratio, the zeolite structure and the activation and calcination conditions, among others. These sites correspond with bridging Si–OH–Al

groups, exhibiting proton-donor Brønsted acidity, and with Lewis electron-acceptor sites connected to the unsaturated coordination of aluminium either bound to the framework or in extra-framework positions [2]. From the ²⁷Al MAS NMR spectra, the framework and extra-framework nature of aluminium present in zeolites can be ascertained, since two peaks centered at ~0 and ~50 ppm, assigned to octahedral and tetrahedrally coordinated aluminium species, respectively, are discerned [3]. Dealumination of the zeolite frameworks, for example by calcination, hydrothermal treatment, or treatment with strong acids makes possible the formation of structural defects and the appearance of extra-framework aluminium species. The acid strength and nature of these different sites can be estimated using adsorption/desorption studies of a variety of probe molecules like CO, hydrocarbons and pyridine and its derivatives, combined with FTIR measurements [4].

On the other hand, aluminium-containing zeolites exhibit unique properties with respect to activity and selectivity. Activity is mostly related to the zeolite acid sites, whereas the shape and size of the micropores may induce various kinds of shape selectivity [5]. A variety of chemical reactions of industrial interest are catalyzed by zeolites, having found application in refinery and petrochemical processes where the shape selectivity properties of the microporous zeolites are exploited [6–10]. However, the location of most

* Corresponding author at: ESCET, Rey Juan Carlos University and IMDEA Energy Institute, c/Tulipán, s/n, 28933, Móstoles, Madrid, Spain. Tel.: +34 91 664 7450.

E-mail addresses: david.serrano@urjc.es, david.serrano@imdea.org (D.P. Serrano).

of the active sites within the micropores produces that zeolite catalysts often suffer from intracrystalline diffusion limitations and steric constraints [11]. To overcome these hindrances, there has been a long-standing drive to either minimize the size of the zeolite crystals, thereby increasing the intercrystalline porosity, or to synthesize novel zeolitic structures with a larger pore size [12]. In this context, zeolites with hierarchical porosity, that is, zeolites featuring multiscale porosity other than microporosity have been found to offer a good solution to this problem [13]. Significant efforts have been devoted to the development of preparation methods for zeolites with a bimodal pore size distribution, such as carbon templating, desilication, zeolite seed assembly, resin templating, recrystallization, mesoscale cationic polymer templating and by using amphiphilic organosilica zeolite precursors [14–22]. Owing to the presence of the hierarchical porous structure, improved diffusion and catalysis properties have generally been observed.

In this work, hierarchical ZSM-5 zeolite obtained by crystallization of silanized protozeolitic units has been employed [22]. This method is based on perturbing the growth of the zeolite crystals by functionalization of the protozeolitic units with organosilanes, in order to prevent their total aggregation. It consists of the following steps: (i) precrystallization of the zeolite synthesis gel with the aim of promoting the formation of zeolite nuclei, (ii) functionalization of the protozeolitic units by reaction with organosilanes, which form a protective organic barrier against aggregation, (iii) crystallization to complete the zeolitization of the functionalized seeds, being subsequently subjected to different calcination procedures. This strategy has led to the synthesis of a variety of zeolites (ZSM-5, ZSM-11, Beta and mordenite) having enhanced both overall and external surface areas [22–25].

Hierarchical zeolites have shown to be very attractive as heterogeneous catalysts for reactions involving bulky molecules, such as polyolefin cracking and the synthesis of chemical intermediates and fine chemicals [23,26]. The latter field constitutes an interesting application as hierarchical zeolites may substitute the homogeneous catalysts conventionally employed.

In a recent work [27], we have concluded that hierarchical ZSM-5 samples, obtained by crystallization of protozeolitic units, present a higher ratio of Lewis/Brønsted sites acid sites, as well as a higher share of extra-framework aluminium, compared with a conventional sample. These results suggested that the nature and coordination of the acid sites located on the non-microporous external surface, or in its vicinity, may exhibit different acidic features and thermal stability. The strength and nature of the acid sites affected both the activity and the selectivity obtained in the different reactions investigated, although the accessibility of the acid sites was another factor playing a key role in the catalytic behaviour of these materials.

In this context, the present work is aimed to investigate how the conditions employed in the calcination treatment, needed to remove the organics present in the as-synthesized materials, influences the acidic and catalytic properties of hierarchical ZSM-5 samples. Thereby, the samples obtained using two different calcinations methods have been tested as catalysts in several fine chemistry reactions: Friedel–Crafts acylation of anisole and 2-methoxynaphthalene, and 1,2-epoxyoctane and isophorone oxide rearrangement. Additionally, the changes induced by these two calcination procedures over the chemical nature and the strength of the acid sites in hierarchical ZSM-5 zeolite have been also studied.

2. Experimental

2.1. Hierarchical zeolite synthesis

Hierarchical ZSM-5 zeolite (h-ZSM-5) was prepared, using tetrapropylammonium hydroxide (TPAOH) as structure directing

agent, from a solution having the following molar composition: $\text{Al}_2\text{O}_3:60 \text{ SiO}_2:11 \text{ TPAOH}:1500 \text{ H}_2\text{O}$ [28]. The precursor solution was precrystallized in a round bottom flask equipped with a condenser under stirring at 90°C for 20 h. Thereafter, phenylaminopropyl-trimethoxysilane (PHAPTMS) was added to the solution in proportion of 5 mol% related to the total silica content of the gel. The final crystallization of the functionalized protozeolitic units was carried out in Teflon-lined autoclaves at 170°C for 7 days [22]. The solid products obtained from the synthesis were separated by centrifugation, washed out with distilled water and dried overnight at 110°C .

A reference ZSM-5 sample was synthesized using the same procedure but omitting the silanization step.

2.2. Calcination treatments

Two different calcination methods were applied to both hierarchical and conventional ZSM-5 samples in order to remove the organics contained in the as-synthesized materials. In the first one the materials were calcined under an air atmosphere increasing the temperature from ambient conditions up to 550°C with a ramp of $1.8^\circ\text{C}/\text{min}$, the final temperature being kept constant for 5 h. The samples so obtained were named as ZSM-5 (air) and h-ZSM-5 (air). In the second calcination treatment, the as-synthesized materials were subjected first to a nitrogen atmosphere increasing the temperature from ambient conditions up to 400°C , remaining at this temperature for 4 h, and followed by a second calcination step under air at 550°C (ramp of $1.8^\circ\text{C}/\text{min}$ and 5 h at the final temperature). The samples so prepared were designated as ZSM-5 (N_2/air) and h-ZSM-5 (N_2/air).

2.3. Characterization

XRD patterns of the different samples were obtained with a Philips X'PERT MPD diffractometer using CuK_α radiation. Argon adsorption–desorption isotherms at -186°C were recorded for the zeolite samples using an Autosorb instrument (Quantachrome). Prior to the measurements, the individual samples were outgassed at 300°C under vacuum. The surface area was determined applying the Brunauer–Emmet–Teller (BET) equation. The pore size distribution was calculated using the adsorption branch of the argon isotherms by applying the NLDFT model (Quantachrome) [29]. The Si/Al atomic ratio of the samples was determined by ICP-AES measurements with a Varian VISTA-AX-CCD equipment. TEM images were obtained in a PHILIPS TECHNAI 20 electron microscope operating at 200 kV. Ammonia temperature programmed desorption (TPD) experiments were carried out in a Micromeritics 2910 (TPD/TPR) equipment.

The coordination of the aluminium atoms in the zeolite samples was determined from the ^{27}Al MAS NMR spectra. They were recorded at 104.26 MHz in a VARIAN Infinity 400 spectrometer at spinning frequency of 4 kHz and intervals ranging from 5 to 30 s between successive accumulations. The external standard reference was $[\text{Al}(\text{H}_2\text{O})_6]^{3+}$ and all measurements were carried out at room temperature. FTIR spectra were recorded with a Bruker Tensor 27 spectrometer. For the pyridine adsorption study, self-supported wafers were prepared and evacuated at 500°C . Then, 2.4 kPa of pyridine (equilibrium pressure) was adsorbed at 170°C . Desorption was subsequently performed at increasing temperatures (250°C , 350°C , 450°C and 520°C) for 20 min each time to determine the acid strength of the sites. Concentration of Brønsted and Lewis acid sites (in $\mu\text{mol}/\text{g}$) were obtained from the experiments of pyridine adsorption, calculated on the basis of the intensity of the 1540 cm^{-1} (pyH $^+$) and 1450 cm^{-1} (pyL) bands, respectively after first desorption step at 250°C and using the respective absorption coefficients, $\epsilon(\text{pyH}^+) = 0.75 \text{ cm}^2/\mu\text{mol}$ and

$\varepsilon(\text{pyL}) = 0.165 \text{ cm}^3/\mu\text{mol}$ [30]. Additional information on the accessibility of the Brønsted acid sites was derived from the adsorption of pivalonitrile and its subsequent desorption for 5 min at room temperature. All measured spectra were recalculated to a 'normalized' wafer of 10 mg (density 3.2 g cm^{-2}).

2.4. Catalytic tests

The acylation reactions were performed under atmospheric pressure in a 250 ml three-necked round bottom flask equipped with a condenser, a thermometer and a magnetic stirrer. In a typical reaction, substrate, acylating agent (acetyl chloride) and solvent (nitrobenzene) were loaded into the reactor. Subsequently, the fresh catalyst was added to the reactor. Samples were taken periodically during 3 h [24]. The activity of the catalysts in the acylation of anisole was tested using the following conditions: anisole/acylating agent = 1 mol/mol, catalyst/anisole = 5 wt.% and $T = 120^\circ\text{C}$. In the acylation of 2-methoxynaphthalene (2-MN), the conditions were as follows: 2-MN/acylating = 1 mol/mol, catalyst/2-MN = 15 wt.% and $T = 180^\circ\text{C}$. Products were analyzed by capillary gas chromatography in a Varian 3900 Series instrument equipped with a $30 \text{ m} \times 0.25 \text{ mm}$ capillary column (CP SIL 8 CB), and a FID detector.

The epoxide rearrangement reactions were carried out in a 0.1-L stirred batch autoclave, equipped with a temperature controller and a pressure gauge under stirring (550 rpm) and autogenous pressure. It was provided with a device to feed the epoxide into the Teflon-lined reactor once the reaction temperature was reached. The (toluene) and the catalyst, previously dried overnight at 135°C , are initially placed in the Teflon-lined reactor. The zero time of the reaction is taken when the temperature reaches the setpoint value and the epoxide is loaded into the reactor [31]. The activity of the catalysts in the 1,2-epoxyoctane isomerization was tested using the following conditions: catalyst/epoxide = 8 wt.% and $T = 150^\circ\text{C}$. Likewise, the conditions employed in the isophorone oxide isomerization were as follows: catalyst/epoxide = 16 wt.% and $T = 100^\circ\text{C}$. The reaction products were analyzed with a VARIAN 3800 gas chromatograph equipped with a capillary column (HPFFAP) with dimensions $60 \text{ mm} \times 0.32 \text{ mm}$ and using a flame ionization detector. Identification of the different reaction products was performed by mass spectrometry (VARIAN SATURN 2000) using standard compounds.

Blank experiments, run without any catalyst, performed under the previous detailed conditions did not show any conversion.

3. Results and discussion

3.1. Effect of the calcination treatment on the zeolite physicochemical properties

Two different ZSM-5 zeolites have been employed as parent materials in this work: one hierarchical ZSM-5 sample (h-ZSM-5), prepared by the seed silanization procedure and one nanocrystalline ZSM-5 used as reference. The ZSM-5 reference sample has been obtained using the same synthesis conditions as for the h-ZSM-5 but omitting the seed silanization treatment. For both materials, the calcination procedure was carried out by two different methods: one-step air calcination and two-step (nitrogen-air) calcination. The first one is a direct calcination traditionally employed for the removal of the structure-directing agent in zeolites. This is a simple treatment, although it may affect negatively the properties of the material since the combustion of the template is a highly exothermic process, which may lead to the appearance of hot spots. The second one is aimed to reduce the potential damage of the sample caused by the formation of these hot spots. Thereby, a first step at 400°C is carried out under a nitrogen atmosphere, so

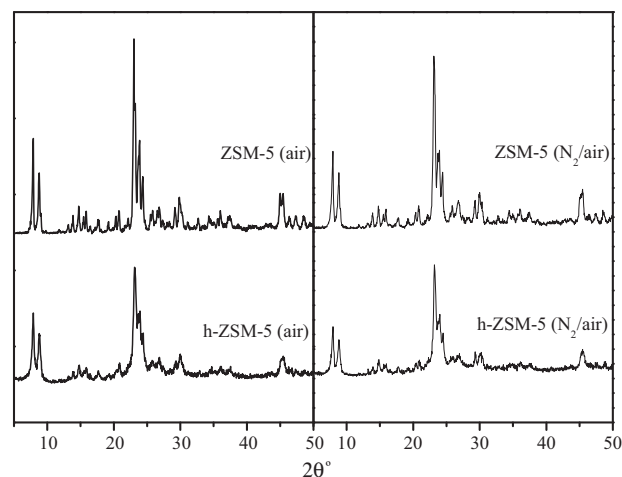


Fig. 1. XRD patterns of both hierarchical and standard ZSM-5 samples.

a great part of the organics contained in the material are removed by an endothermic decomposition process instead of by combustion. In the second step, both the organic matter and the carbon residues, still present in the sample, are removed by shifting to an air atmosphere and increasing the temperature up to 550°C .

All the materials present high crystallinity, as confirmed by the XRD diffractograms depicted in Fig. 1, showing the typical pattern of the MFI zeolitic structure. However, the samples prepared using the seed silanization treatment, h-ZSM-5 samples, disclose peaks less intense and broader than those corresponding to the conventional zeolite. This is an earlier observed result, being accounted by the smaller size of the crystalline domains in the hierarchical zeolites obtained from silanized protozeolitic units. On the other hand, the calcination procedure seems not to have any significant effect on the relative crystallinity of the samples. Thus, for both types of ZSM-5 materials (hierarchical and standard ones), the intensity of the XRD peaks is very similar for the samples obtained using different calcination treatments.

The textural properties of the samples have been determined from argon adsorption–desorption isotherms. The use of Ar instead of N_2 allows the pore size distribution to be obtained as a continuous curve for a wide range of pore sizes by employing the NLDFT model, as well as to distinguish the contribution of the different levels of porosity present in these samples to both the overall surface area and the pore volume. The argon adsorption isotherms of the different ZSM-5 samples investigated in this work are represented in Fig. 2. The isotherm of the reference sample is typical of microporous solids with a high adsorption at low relative pressures. In addition, it also shows a significant adsorption at

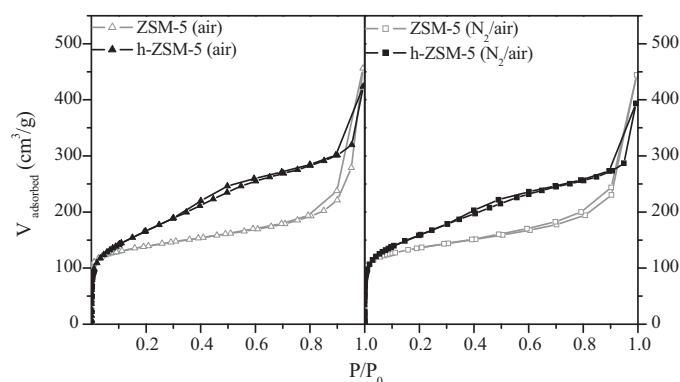


Fig. 2. Ar adsorption–desorption isotherms at 87 K of the ZSM-5 samples.

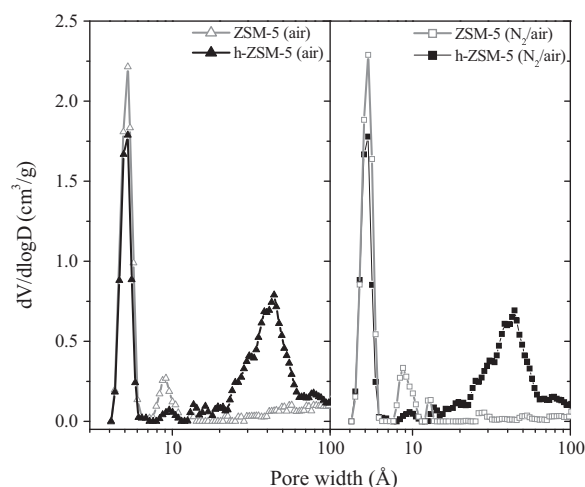


Fig. 3. NLDFT pore size distributions of the ZSM-5 samples.

high relative pressures, denoting the presence of intercrystalline porosity. In the case of the hierarchical zeolites, the Ar adsorption takes place at both low and intermediate relative pressure. The latter has been assigned to the voids existing between different crystalline nanounits [22,27], which are generated and enhanced by the silanization agent, which acts as a barrier during the growth of the zeolite crystals, hindering their complete densification.

This result is confirmed by the pore size distribution derived from the argon isotherms by applying the NLDFT model (see Fig. 3). In addition to the peak corresponding to the ZSM-5 micropores, the hierarchical samples possess a second type of porosity with sizes in the range 20–70 Å. The shape and relative contribution of this second peak are not significantly modified by changing the calcination conditions.

These results are also in agreement with the slight variations in the textural properties of the samples, as it is denoted in Table 1. According to previous works, the hierarchical samples show enhanced BET and external surface areas. The latter include all the non-microporous surface area of the samples, with contributions coming from both the mesopores and the outer part of the particles. On the other hand, for both hierarchical and reference ZSM-5, only small variations can be observed in the value of the textural properties when employing different calcination treatments. Nevertheless, it is noteworthy to point out the enhanced textural properties displayed by the hierarchical h-ZSM-5 samples, in comparison with the reference ZSM-5 materials, regardless of the template removal procedure. The external surface area of the reference ZSM-5 shows a relatively large value (96 and 83 m²/g, under air and N₂ atmosphere calcination, respectively), due to its nanocrystalline character, although the value of this parameter is strongly increased for the hierarchical ZSM-5 material, reaching 323 and 336 m²/g, respectively.

TEM micrographs of the different ZSM-5 samples are illustrated in Fig. 4. Single crystals with sizes higher than 50 nm are observed for the material prepared omitting the seed silanization treatment. In contrast, aggregates with sponge-like morphology and diameters around 200 nm are obtained for the organofunctionalized sample. These aggregates are constituted by very small nanounits with sizes even below 10 nm. Although not shown in this figure, no significant differences are observed when comparing the size of the crystals, nanounits and particles of the samples prepared using different calcination methods. Therefore, it can be concluded that the calcination treatments here employed do not lead to important changes in the nanoscale properties of the samples.

In order to bear out the coordination of the aluminium present in the samples, they were analyzed by ²⁷Al MAS NMR, the results so obtained being shown in Fig. 5. In all cases, the spectra of the parent material are compared with those of the samples obtained using different calcination treatments. For the as-synthesized materials, just one signal is detected centered at 50 ppm, indicating that all the Al atoms exhibit a tetrahedral coordination and that they are incorporated into the zeolite framework. In contrast, the samples obtained after calcination shows two clear peaks centered at ~0 and ~50 ppm originating from octahedrally and tetrahedrally coordinated aluminium species, respectively. The peak at 0 ppm denotes that a part of the framework Al has been extracted during the calcination treatment leading to extra-framework species with octahedral coordination. This effect is more pronounced for the hierarchical ZSM-5, showing that the Al located outside the zeolite micropores, or in the vicinity of the micropore mouths, is less stable during the calcination treatment. Nevertheless, it is remarkable that even so most of the Al atoms keep the tetrahedral coordination in h-ZSM-5 after the calcination, with similar values being observed for both calcination methods. This behaviour is also denoted for the reference ZSM-5 material.

The above commented results point out that the calcination treatment does not change the proportion of framework/extra-framework aluminium, but this parameter is really related to the share of non-microporous surface area. However, the calcination treatment has a pronounced effect on the uniformity of aluminium environments, which can be derived from the full-width-at-half-maximum (FWHM) values of the signal centered at 50 ppm in the ²⁷Al MAS-NMR spectra [32]. When comparing both parent materials, it is observed that the FWHM value is larger in the hierarchical ZSM-5 than in the reference sample. This is consistent with previous results, and it has been assigned to a higher variety of environments for the Al atoms located in tetrahedral positions of the external zeolite surface. The latter can be considered as an imperfection of the zeolite structure, which provides more variability for the bond distances and angles of the Si and Al species there located. Interestingly, the value of the FWHM parameter is strongly influenced by the calcination conditions. For both h-ZSM-5 and reference ZSM-5 materials, the FWHM value increases after calcination, since this treatment causes a significant distortion in the local environment of the Al atoms. Moreover, in both cases the

Table 1
Physicochemical properties of the samples.

	S_{BET}^a (m ² /g)	S_{EXT}^b (m ² /g)	$V_{\mu\text{pore}}^b$ (cm ³ /g)	Si/Al ^c	T_{max}^d (°C)	Acidity ^d (mmol/g)	C_{Bronsted}^e (mmol/g)	C_{Lewis}^e (mmol/g)
ZSM-5 (air)	431	96	0.208	31	357	0.4259	0.410	0.061
h-ZSM-5 (air)	524	323	0.125	33	349	0.3660	0.209	0.141
ZSM-5 (N ₂ /air)	418	83	0.210	30	356	0.4126	0.402	0.053
h-ZSM-5 (N ₂ /air)	539	336	0.126	33	344	0.3742	0.285	0.139

^a Argon isotherms.

^b $S_{\text{EXT}} = S_{\text{BET}} - S_{\mu\text{pore}}$ (NL-DFT), $V_{\mu\text{pore}}$ (NL-DFT).

^c ICP-AES.

^d NH₃-TPD.

^e Pyridine adsorption-IR.

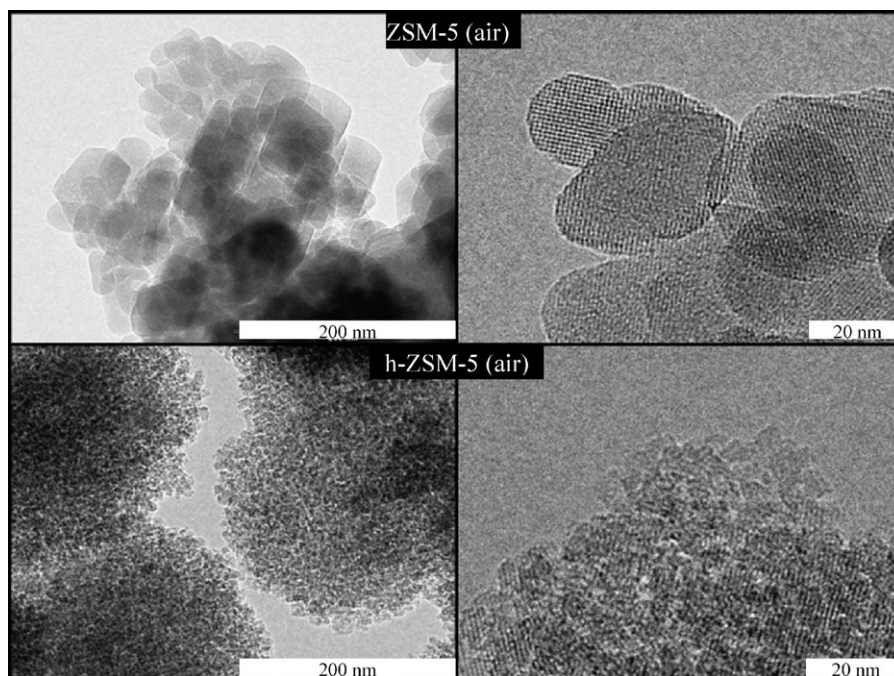


Fig. 4. TEM images of ZSM-5 (air) and h-ZSM-5 (air) samples.

FWHM increase is less important when using two-step calcination, showing that the latter is more effective in preserving the original state of the Al atoms with tetrahedral coordination. Thus, for the h-ZSM-5 material, the FWHM value for the 50 ppm peak (tetrahedral coordination) increases from 7.22 ppm in the parent hierarchical zeolite to 7.82 ppm when using a nitrogen/air calcination. However, this variation is quite larger (up to 8.63 ppm) when h-ZSM-5 is subjected to direct air calcination, showing that the local environment of the Al species located on the external surface (non-microporous surface) is very sensitive to the calcination conditions. Such broadening can also be related to the presence of Si(OH)Al groupings at the surface of the mesopores as it will be further explained on the basis of the IR studies of pyridine desorption.

The use of different calcination methods may also affect the acid properties of the zeolites, which in turn are essential to explain their catalytic performance. A gross assessment of the acid features of ZSM-5 zeolite can be carried out by using ammonia temperature programmed desorption measurements (ammonia TPD). The results obtained in the application of this technique to the samples investigated in this work are summarized in Table 1. The acidity of the hierarchical samples is slightly lower compared to that of the reference materials, in terms of both acid strength (temperature of the peak maximum in the ammonia TPD) and amount of acid sites being detected. These results are consistent with previous works, showing that the generation of hierarchical porosity leads to a small reduction in the acidic features of ZSM-5 zeolite. No great changes are observed among the samples when evaluating the effect of the calcination treatment. In the case of the h-ZSM-5 material, the sample obtained using a two-step calcination shows a slightly lower acid strength but higher number of acid sites than the sample calcined directly in air. This apparent discrepancy will be further explained on the basis of the IR spectroscopy of pyridine desorption. Additionally, it must be taken into account that ammonia TPD is not a very sensitive technique for detecting changes in the zeolite acidity and that it cannot distinguish between nature and type of acid sites.

Accordingly, the acidic properties of the samples have been also investigated by adsorption of pyridine, used as probe molecule, followed by FTIR spectroscopy. Pyridine adsorption on

the investigated samples led to the appearance of new absorption bands corresponding to pyridine interacting with Brønsted (1545 cm^{-1}) and Lewis acid sites ($1445\text{--}1465\text{ cm}^{-1}$). Fig. 6 depicts the FTIR spectra of pyridine adsorbed on the samples and subsequently evacuated at different temperatures (170, 250, 350, 450 and 520°C), which causes a progressive desorption of pyridine. These measurements are very useful in characterizing the zeolite acid properties as it is possible to distinguish between Brønsted and Lewis acid sites, giving also information about their acid strength from the adsorbed pyridine evolution with the temperature increase.

The results obtained in terms of acid sites concentration, after desorption at 170°C , are included in Table 1. Independently of the calcination treatment, the reference ZSM-5 samples show a quite higher concentration of Brønsted acid sites compared to the hierarchical materials, while the opposite is observed for the Lewis site concentration. This fact may be at least partially assigned to the higher proportion of extra-framework Al species detected in the hierarchical samples by ^{27}Al MAS NMR, which should act as

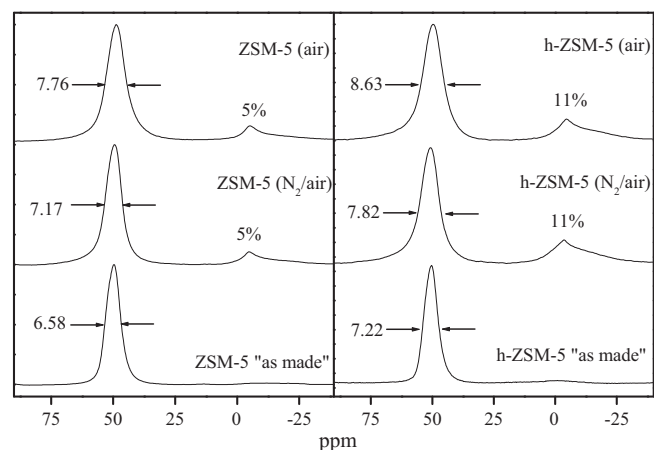


Fig. 5. ^{27}Al MAS NMR spectra of the parent ZSM-5 materials and after different calcination treatments.

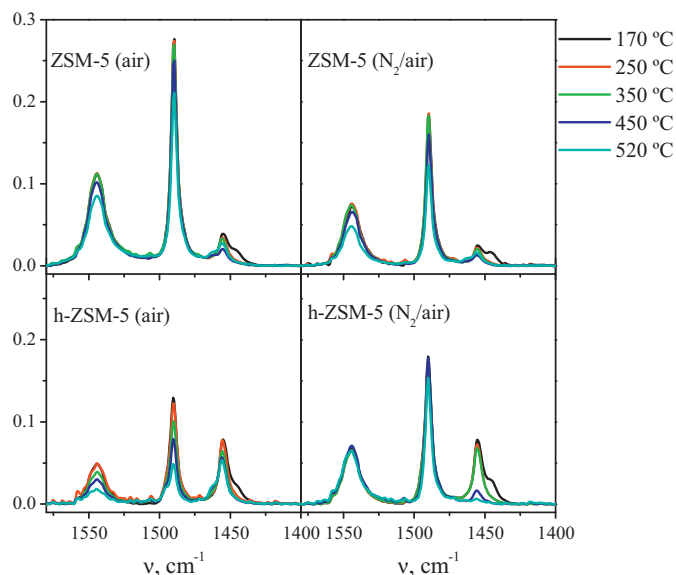


Fig. 6. FTIR spectra of the samples after pyridine adsorption and evacuation at different temperatures (spectra at 170 °C and normalized to a standard 10 mg mass).

Lewis acid sites. However, this is not enough for accounting the high concentration of Lewis sites present in the hierarchical ZSM-5 samples, suggesting that also a part of the framework Al is related to these type of acid sites. This situation is quite common, as in many publications zeolitic samples without any extra framework aluminium presence displayed Lewis acidity when measured by IR technique.

On the other hand, a strong effect of the calcination conditions is observed for the Brønsted sites population in the h-ZSM-5 material. This parameter is quite larger in the samples obtained using a two-step calcination, which may be in agreement with the higher uniformity of Al environments denoted in this sample from the FWHM values. Moreover, when the evolution of the Brønsted sites concentration with the pyridine evacuation temperature (see Fig. 7) is considered, great differences are observed in their strength for

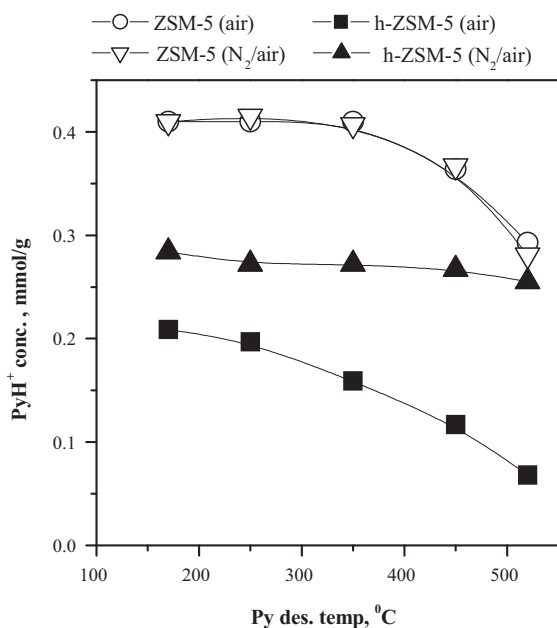


Fig. 7. Evolution of the pyridine adsorbed on Brønsted acid sites of the different samples as the evacuation temperature is increased.

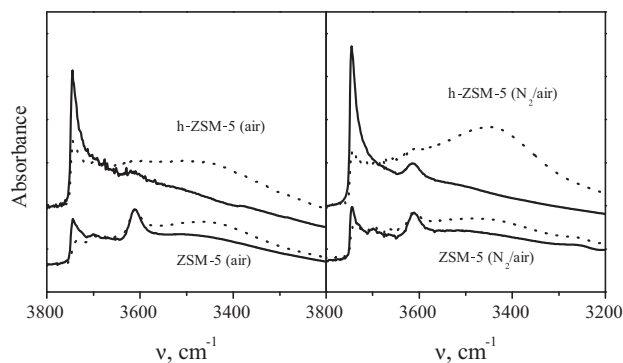


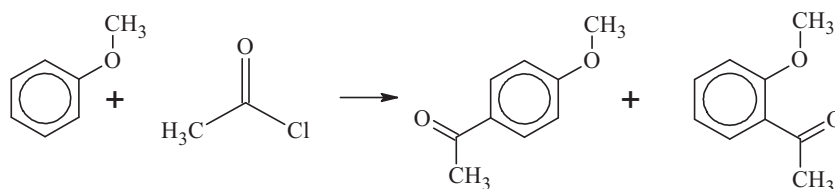
Fig. 8. IR spectra of OH groups in ZSM-5 zeolites before (—) and after (···) pivalonitrile adsorption, followed by 5 min evacuation at ambient temperature.

the two hierarchical ZSM-5 samples. Thus, while for the sample obtained by direct air calcination a high pyridine desorption ratio is observed, the sample calcined following a two-step method is capable of retaining adsorbed a great part of the pyridine. These results indicate that the two-step calcination also influences positively the strength of the Brønsted acid sites in hierarchical ZSM-5.

NH₃-TPD method is suitable to follow the total behaviour of acidic sites, while pyridine thermal desorption method can discriminate between Brønsted and Lewis acidity. The fact that during thermal desorption pyridine is desorbed from Lewis acid sites of h-ZSM-5 (air) at very high desorption temperature may explain why by NH₃-TPD this sample appeared stronger acidic than the h-ZSM-5 (N₂/air). In the latter zeolite the majority of pyridine coordinated to the Lewis sites was desorbed at 450 °C.

It is also worth to note that during pyridine desorption the intensity of pyridinium ion is decreasing but, at the same time, this is not accompanied by the increase of the intensity of the Si(OH)Al groups. Such fact has already been observed in the case of the formation of the secondary mesoporous system in ZSM-5 zeolites due to desilication [33]. It was proposed that some Si(OH)Al groups may have been formed on the surface of mesopores, having properties that may be comparable to those of the hydroxyls existing either in mesoporous materials of M41S family [34] or of ITQ-2 material [35]. It is known that such OH groups are characterized by unusually low absorption coefficient, therefore being practically invisible for IR spectroscopy. In addition, their acid strength is also deeply lowered. Thus, the presence of the weak Brønsted sites from the mesopores may also contribute to the lowered acid strength of hierarchical zeolites.

Some of the results, obtained during catalytic test reactions may be also explained by the enhanced accessibility of the Si(OH)Al groups from the mesoporous domain. Application of pivalonitrile as a probe molecule for testing external acidity of zeolites was proven useful by the group of Busca [36]. The presence of *tert*-butyl group prevents entrance into the 10-ring openings and therefore restricting any interaction to the external surface of the MFI-type zeolites. Therefore, pivalonitrile interacts only with a fraction of the OH groups, which are those located on the external surface or in the vicinity of the pore entrances, while does not interact with the OH groups located well inside the micropore system. As shown in Fig. 8, Pivalonitrile interacts only with a small fraction of Si(OH)Al groups in non-hierarchical ZSM-5, independently of the calcination method, but with the majority of these groups in both hierarchical zeolites. This result, together with the presence of weak Brønsted centers inside the generated mesopores, indicates that these materials present singular acidic properties, which makes them potentially interesting catalysts to be probed in a variety of reactions involving bulky molecules.



Scheme 1. Anisole acylation.

3.2. Catalytic performance in acylation reactions

The influence of the calcination procedure in the catalytic behaviour of the hierarchical and reference ZSM-5 samples has been studied through the synthesis of aryl ketones by means of the Friedel–Crafts acylation. Different authors [37,38] have reported the use of solid catalysts in acylation reactions of arenes, aromatics ethers, aromatic thioethers, phenolic substrates and heterocycles, showing the delicate balance between the Lewis and Brønsted acid sites in determining their activity in this type of reactions. In the present work, anisole and 2-methoxynaphthalene (2-MN) acylation have been selected in order to check the catalytic performance of both reference and hierarchical zeolite samples with substrates having different molecular sizes.

The acylation of anisole was investigated using acetyl chloride as acylating agent. From this reaction an aryl ketone, the p-methoxyacetophenone (p-MAP), is obtained as product of interest in fine chemistry (Scheme 1). The selectivity towards p-MAP was 97% for all the catalysts tested, remaining constant throughout the reaction.

Fig. 9 illustrates the anisole conversion as a function of reaction time for the different catalysts tested. At any time, the conversions obtained over the reference ZSM-5 sample were remarkably lower than those corresponding to the hierarchical materials, reaching a plateau at around 10%. This result evidences the limitations that the anisole molecule undergoes for accessing to the acid sites of the reference ZSM-5 zeolite due to the small size of its micropores, despite being a nanocrystalline sample with a considerable ratio of external surface area [39]. In contrast, steric and diffusional hindrances are lowered in a high extension in the case of the hierarchical ZSM-5 samples, due to the presence of the secondary mesoporosity.

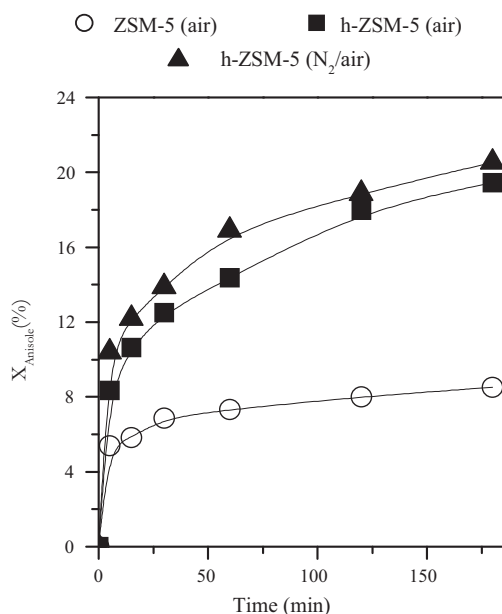


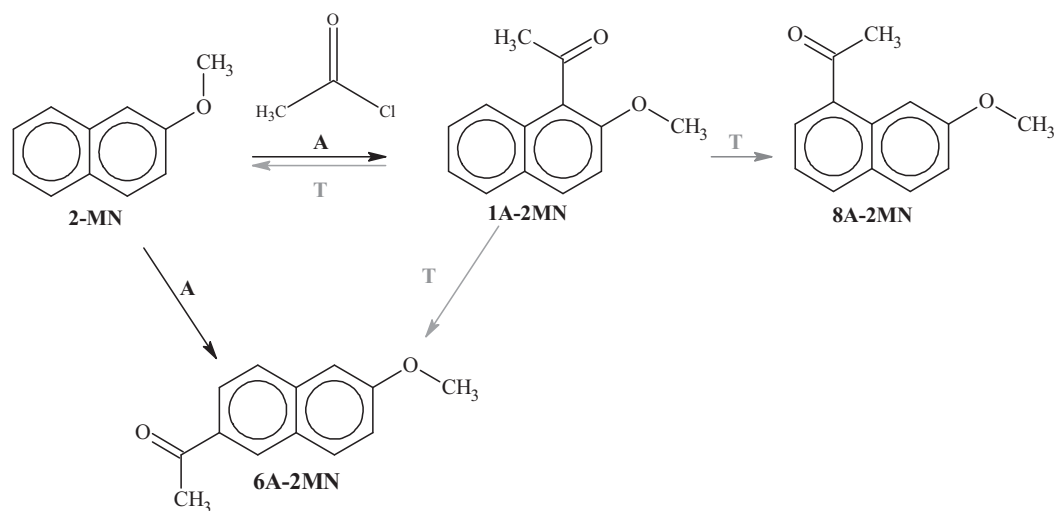
Fig. 9. Evolution of the anisole conversion with the reaction time.

These results confirm the positive effect of the hierarchical porosity on the acylation reaction by increasing the accessibility of the anisole molecule to the active sites of the hierarchical ZSM-5 zeolite. Additionally, the h-ZSM-5 (N₂/air) sample exhibits a slightly higher anisole conversion than hierarchical zeolite treated under air atmosphere. Although the contribution of the Lewis acidity in this reaction must not be ruled out, this fact suggests the positive effect of the higher concentration of strong Brønsted acid sites, which are present in this sample as a result of the calcination conditions.

One of the most frequently studied acylating reaction is the acylation of 2-methoxynaphthalene (2-MN), which has been earlier investigated over different types of solid catalysts [40]. In the present work, 2-MN was selected, due to its higher molecule size, to study the catalytic properties of the ZSM-5 zeolite samples [41]. The reaction was also performed employing acetyl chloride as acylating agent (Scheme 2). When using 2-MN, a major complexity is introduced, compared to anisole, since three isomer reaction products may be formed: 1-acetyl-2-methoxynaphthalene (1A-2-MN), 8-acetyl-2-methoxynaphthalene (8A-2-MN) and 6-acetyl-2-methoxynaphthalene (6A-2-MN). The latter is the desired product, since it is an intermediate of the anti-inflammatory Naproxen. Moreover, at long reaction times, 1A-2-MN may be converted via intra and intermolecular transacylation into 6A-2-MN and 8A-2-MN (Scheme 2) [42]. Large pore zeolites, particularly zeolite Beta, have been reported to be capable of discriminating between these products owing to their different sizes [24]. As a consequence of these secondary reactions, the product distribution, and accordingly the selectivity towards the desired product, may change along the reaction time. Therefore, the rate of 2-MN acylation and the products distribution is expected to depend greatly on the textural and acidic properties of the catalysts [43].

Fig. 10 displays the evolution of the catalytic activity in 2-MN acylation for both reference ZSM-5 (air) sample and the hierarchical zeolites calcined under the two different treatments. Hierarchical zeolites lead to greater 2-MN conversions than that obtained with the nanocrystalline zeolite used as reference. These results confirm again the remarkable effect of the presence of high external surface area and secondary porosity in the hierarchical zeolites, which lower the steric and diffusional hindrances compared with the reference ZSM-5 sample.

Regarding the two hierarchical zeolites, no substantial differences in terms of conversions are noticed when changing the calcination procedure, with just slightly higher values for the h-ZSM-5 (N₂/air) sample. However, important differences were observed in the product distribution. At short reaction times, formation of 1A-2MN is favored with respect to 6A-2MN, the greatest yields being obtained with the hierarchical ZSM-5 samples. With the progress of the reaction, the 1A-2MN yield reaches a maximum, which confirms the participation of this compound in intra- and intermolecular side reactions. This has a direct and positive impact on the 6A-2MN yield, as it may be formed by both direct acylation of 2-MN and transacylation of 1A-2MN. In this way, it is important to note that the hierarchical ZSM-5 sample, calcined under nitrogen/air atmosphere, provides higher yields into 6A-2MN products than the h-ZSM-5 (air) material. This interesting result may be



Scheme 2. 2-MN acylation reaction scheme.

related to the higher concentration of Brønsted acid sites present in h-ZSM-5 (N_2 /air), assuming that they facilitate the transacylation side reaction of 1A-2MN into 6A-2MN.

3.3. Catalytic properties in epoxide rearrangements reactions

The catalytic behaviour of the zeolites synthesized in this work has been also investigated in the liquid phase rearrangement of epoxides. As substrates, two epoxides with different geometrical configuration and molecular size, and having commercial applications in fine chemistry, have been selected to probe the influence of the calcination: 1,2-epoxyoctane (linear epoxide), and isophorone oxide (cyclic epoxide) [44,45].

The isomerization of linear 1,2-epoxyoctane, illustrated in Scheme 3, may yield two types of commercially interesting compounds. The first one is the aldehyde, which can be conveniently transformed into carboxylic acids or terminal alcohols, important precursors in organic chemistry [46]. The second type corresponds with octenols, which can be also selectively hydrogenated to linear alcohols [47]. In addition, secondary reactions may occur through aldol condensation reactions [44]. The catalytic rearrangement of this epoxide has been widely studied over a variety of solid catalysts [31] with different structural features and acid properties, including amorphous, mesostructured and zeolitic catalysts. Al-containing

zeolitic materials, such as ZSM-5, are known to be active in the rearrangement of 1,2-epoxyoctane, although often with limited selectivity towards the desired products. Moreover, the extension of the reaction seems to be dramatically influenced by the pore size constraints. Thus, Al-containing mesostructured materials, such as Al-MCM-41, present much higher activity than zeolitic catalysts, which has been assigned to their larger pore size. The fact that ZSM-5 contains mainly Brønsted acid sites whereas Al-MCM-41 is featured by Lewis acidity indicates that both types of acid centers are active in the liquid phase isomerization of 1,2-epoxyoctane [48]. The extension of the reactions shown in Scheme 3, and consequently the relative proportion of the different products, are expected to depend strongly on the textural and acidic properties of the catalysts employed in 1,2-epoxyoctane isomerization.

Fig. 11 displays, as a function of the reaction time, the 1,2-epoxyoctane conversion obtained with the hierarchical ZSM-5 samples and the reference ZSM-5 (air). Regardless the calcination method, hierarchical zeolites present remarkably higher activity than the reference sample. This may be assigned also in this case to the enhanced accessibility of the substrates to the active sites caused by the hierarchical porosity. Moreover, the h-ZSM-5 (N_2 /air) sample exhibits clearly higher conversions than h-ZSM-5 (air). Since in terms of textural properties and secondary porosity both hierarchical samples are quite similar, this difference must

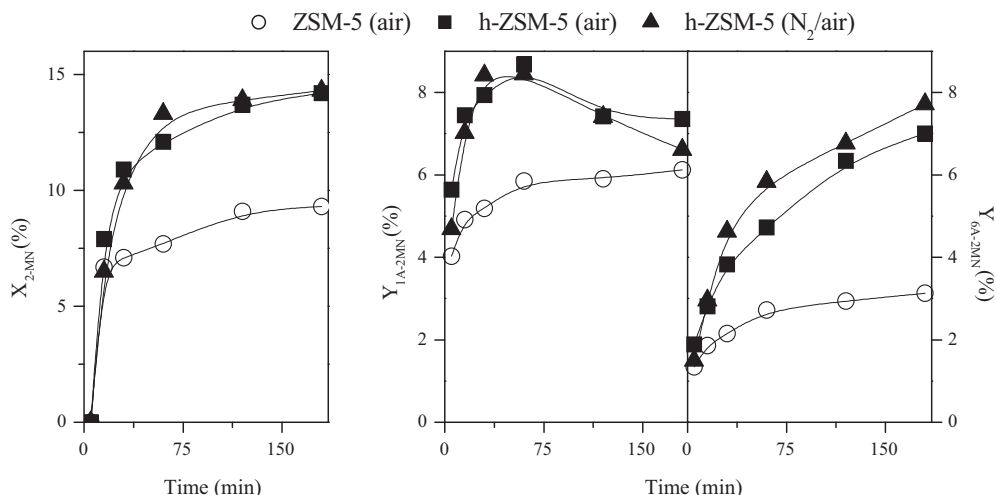
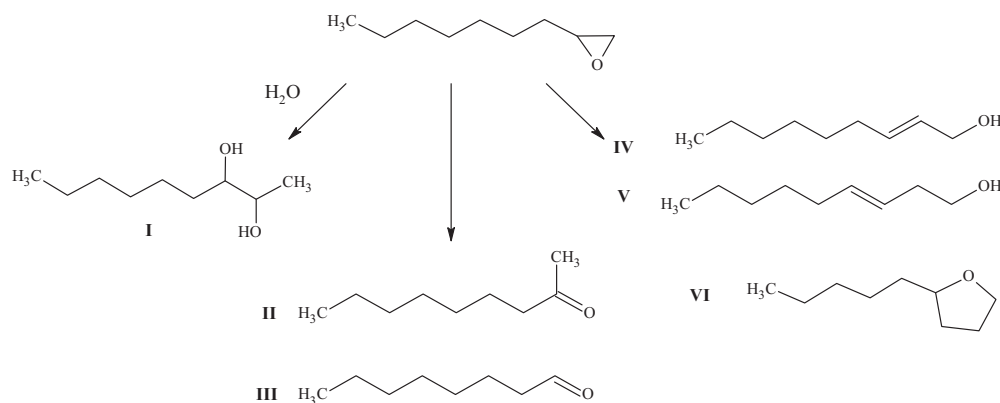


Fig. 10. 2-MN acylation: conversion (left) and 1A-2MN and 6A-2MN yields (right).



Scheme 3. Products obtained in isomerization of 1,2-epoxyoctane: 1,2-octanediol (I), 2-octanone (II), octanal (III), 2-octen-1-ol (IV), 3-octen-1-ol (V) and 2-butyltetrahydrofuran (VI).

be related to the presence of a higher population of Brønsted acid sites with high strength in the sample calcined following a two-step method.

In regard to the product distribution, the hierarchical samples show higher yields towards both octanal and octenols than the reference zeolite. Moreover, for the hierarchical zeolites, the calcination method presents no influence on the octanal yield. The Lewis acidity seems to be relevant in the octanal formation, as shown by the fact that the hierarchical samples (whatever the calcination treatment) exhibit higher octanal yield than the reference ZSM-5. As reported in the literature, aldehyde formation is mainly favored by the use of weak acids, which may be related with the lower overall acid strength and the higher Lewis acidity present in the hierarchical zeolites. On the other hand, large differences between both hierarchical samples can be observed in terms of octenols yield, its value being quite higher for the h-ZSM-5 (N_2 /air) sample. This result must be interpreted taking into account the differences in acidity existing between these two samples. Accordingly, the Brønsted acid sites, present in the h-ZSM-5 (N_2 /air) sample in a higher concentration, seem to play a predominant role in catalyzing the 1,2-epoxyoctane isomerization into octenols. The reason could be that the epoxide rearrangement of epoxides into octenols follows a complex mechanism, involving the formation of both double bond and alcohol groups, which is more easily catalyzed by Brønsted sites due to its higher strength and lower steric impediments compared to Lewis centers.

Finally, isophorone oxide (IO) was employed as a cyclic substrate for testing the catalytic properties of the samples. The reaction mechanism [49] is illustrated in Scheme 4, resulting in the formation of three compounds: 3,5,5-trimethyl-1,2-cyclohexanedione (I), 2-formyl-2,4,4-trimethylcyclopentanone (II) and 2,4,4-trimethylcyclopentanone (III). From an industrial standpoint, the desired compound is the keto-aldehyde (II), an interesting intermediate for the synthesis of other cyclopentanone derivatives with floral and fruity smells and used as fragrances [47]. The acid-catalyzed reaction mechanism leading to the synthesis of keto aldehyde (II) has been discussed for homogeneous catalysts [50]. Likewise, it is of interest to know how the product distribution is changed in the presence of heterogeneous catalysts and also whether the decarbonylation of compound (II) to compound (III) can be suppressed. In the present work, this reaction has been also applied to check the influence of both the hierarchical zeolite and the calcination treatment.

Fig. 12 represents the evolution of the conversion and the yield into the desired product along the reaction time. Once again, a higher activity is obtained in the rearrangement of isophorone oxide over the hierarchical samples, which may be attributed to their improved accessibility, as a consequence of the generated extra-porosity, in regard to the reference material. Comparing the hierarchical zeolites, the sample calcined under nitrogen and afterwards under air atmosphere shows a higher conversion, and also a higher yield into the desired product. As it occurred in others

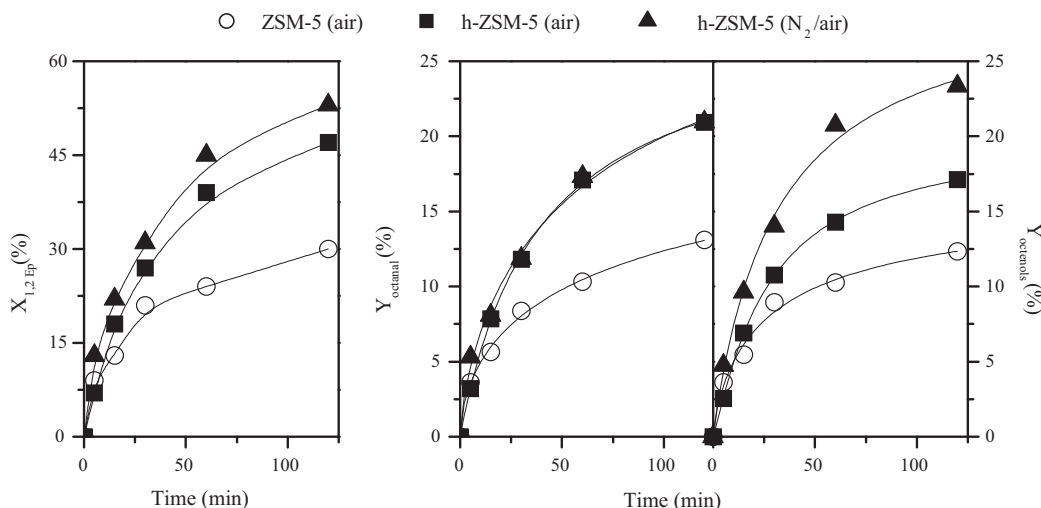
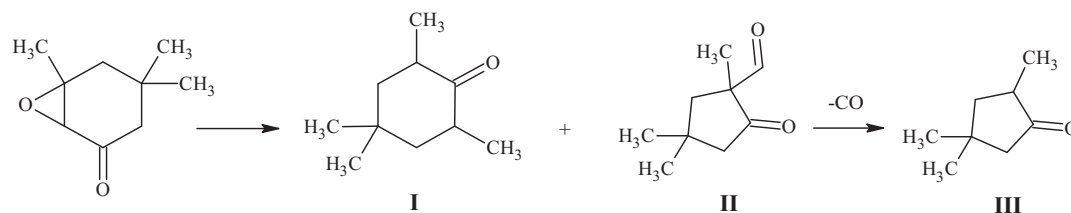


Fig. 11. 1,2-epoxyoctane isomerization: conversion (left) and octanal and octenols yield (right).



Scheme 4. Products obtained in isomerization of isophorone oxide: 3,5,5-trimethyl-1,2-cyclohexanedione (I) and 2-formyl-2,4,4-trimethylcyclopentanone (II) and subsequent deformylation of (II) to 2,4,4-trimethylcyclopentanone (III).

of the reaction here studied, this difference can be interpreted as a positive effect of the higher concentration of Brønsted acid sites in h-ZSM-5 (N_2 /air), which have been preserved during the two-step calcination of this sample. In this case, no great changes were observed among the samples in terms of the selectivity towards the three reaction products [51]. The acyl migration is favored, resulting in ring contraction and consequently in the formation of the aldehyde, which leads to selectivities towards II over 80%.

The above results indicate that accessibility is an important aspect that must be considered for understanding the catalytic properties of zeolites in the presence of steric and/or diffusional constraints. In this way, the main advantage of hierarchical zeolites compared to standard ones is to exhibit an improved accessibility to the active sites, which is especially important when processing bulky molecules. However, in addition to accessibility, it must be taken into account that both Brønsted and Lewis acid sites are responsible of the catalytic activity shown by hierarchical ZSM-5 in the reactions investigated in this work: aromatic acylation and epoxide rearrangement. However, this does not mean that the intrinsic activity of Brønsted and Lewis sites is necessarily the same, but it may depend on the specific characteristics of each reaction. Thus, for the hierarchical ZSM-5 zeolite, it is observed that the sample prepared by a controlled calcination treatment possesses higher content of Brønsted acid sites, which clearly reverberate in the highest catalytic activity exhibited by this hierarchical ZSM-5 zeolite. This suggests that Brønsted acidity shows a higher intrinsic activity than the Lewis one, at least in the reactions here studied, although it does not imply that the Lewis acidity has no effect and, therefore, its contribution cannot be ruled out to explain the catalytic properties.

In summary, the combination of hierarchical porosity with a controlled calcination treatment allows ZSM-5 materials to be obtained showing a high accessibility and preserving largely the

typical Brønsted acidity of this material, which in turn results in improving their catalytic properties in both aromatic acylation and epoxide rearrangement reactions.

4. Conclusions

The effect of the calcination treatment on the zeolite physico-chemical properties and its catalytic performance is studied on this work. Two different ZSM-5 zeolites are employed, one hierarchical ZSM-5 sample (h-ZSM-5), prepared by the seed silanization procedure and one nanocrystalline ZSM-5 used as reference. For both materials, the calcination procedure is carried out by two different methods: one-step air calcination and two-step (nitrogen/air) calcination. Clear differences are noticed related to the textural properties of the two ZSM-5 samples. Thus, h-ZSM-5 presents not only higher BET surface area than standard ZSM-5 zeolite, but the majority of it is shared by surface located outside the zeolite micropores.

FTIR studies show almost no differences between the acidic properties of the conventional zeolite calcined by both methods. However, noticeable changes are observed over the hierarchical ZSM-5 material. Thus, the concentration of Brønsted acid sites decreases by half in the case of one-step air calcination, but only a quarter when using two-step nitrogen/air calcination. These changes in the acidic properties denote that the aluminium present in hierarchical ZSM-5 is very sensitive to the calcination conditions and may suffer framework extraction and dehydroxylation when the calcination is performed directly in air.

Regarding the catalytic features, hierarchical materials, prepared by crystallization of silanized protozeolitic units, disclose higher activity than the reference ZSM-5 zeolite in the type of reactions here investigated Friedel–Crafts acylation and epoxide rearrangement. In addition, the hierarchical ZSM-5 zeolite, calcined by a two-step (nitrogen/air) treatment, exhibits in all cases higher conversions and product yields than the hierarchical ZSM-5 directly calcined in air. These results are assigned to the higher concentration of Brønsted acid sites with high acid strength existing in the former sample, as they are better preserved when the calcination treatment is carried out using a two-step method, although the role of Lewis acidity in these reactions cannot be ruled out.

Finally, it can be concluded that the combination of hierarchical porosity with a controlled calcination treatment allows ZSM-5 materials to be obtained showing a high accessibility and preserving largely the typical Brønsted acidity of this material. The combination of both factors results in improving their catalytic properties in a variety of reactions, such as aromatic acylation and epoxide rearrangement.

Acknowledgment

The financial support of the Spanish government (CTQ2005-09078/PPQ and CTQ2008-05909/PPQ) is gratefully acknowledged.

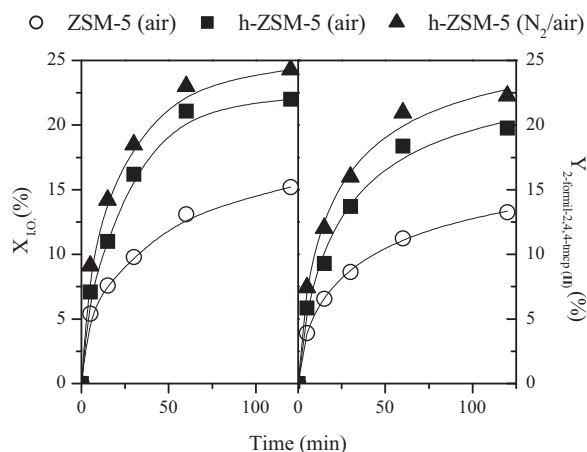


Fig. 12. Isophorone oxide isomerization: conversion (left) and 2-formyl-2,4,4-trimethylcyclopentanone yield (right).

References

- [1] A. Corma, Chem. Rev. 95 (1995) 559.
- [2] P.A. Jacobs, Carboniogenic Activity of Zeolites, Elsevier, Amsterdam, 1977.
- [3] G. Engelhardt, D. Michel, High-Resolution Solid-State NMR of Silicates and Zeolites, Wiley, New York, 1987.
- [4] J. Cejka, B. Wichterlova, Catal. Rev. 44 (2002) 375.
- [5] C.R. Marcilly, Top. Catal. 13 (2000) 357.
- [6] M. Hartmann, Angew. Chem. Int. Ed. 43 (2004) 5880–5882.
- [7] N.Y. Chen, W.E. Garwood, F.G. Dwyer, Shape Selective Catalysis in Industrial Applications, Marcel and Dekker, New York, 1996.
- [8] N. Viswanadham, G. MuraliDhar, M.O. Garg, Int. J. Oil Gas Coal Technol. 1 (1/2) (2008).
- [9] P.-S.E. Dai, Catal. Today 26 (1995) 3.
- [10] C.H. Christensen, K. Johannsen, E. Törnqvist, I. Schmidt, H. Topsøe, C.H. Christensen, Catal. Today 128 (2007) 117.
- [11] J. Kärger, D.M. Ruthven, Diffusion in Zeolites and Other Microporous Materials, John Wiley and Sons, New York, 1992.
- [12] S. Van Donk, A.H. Janssen, J.H. Bitter, K.P. de Jong, Catal. Rev. 45 (2003) 297.
- [13] M.S. Holm, E. Taarning, K. Egeblad, C.H. Christensen, Catal. Today 168 (2011) 3.
- [14] C.J.H. Jacobsen, C. Madsen, J. Houzvicka, I. Schmidt, A. Carlsson, J. Am. Chem. Soc. 122 (2000) 7116.
- [15] M. Ogura, S.H. Shinomiya, J. Tateno, Y. Nara, E. Kikuchi, M. Matsukata, Chem. Lett. (2000) 882.
- [16] C.C. Pavel, W. Schmidt, Chem. Commun. (2006) 882.
- [17] Y. Liu, T.J. Pinnavaia, J. Mater. Chem. 14 (2004) 1099.
- [18] V. Naydenov, L. Tosheva, J. Sterte, Micropor. Mesopor. Mater. 35 (2000) 621.
- [19] I. Ivanova, A.S. Kuznetsov, O.A. Ponomareva, V.V. Yuschenko, E.E. Knyazeva, Stud. Surf. Sci. Catal. 158 (2005) 121.
- [20] F.S. Xiao, L. Wang, C. Yin, K. Lin, Y. Di, J. Li, R. Xu, D.S. Su, R. Schlögl, T. Yokoi, T. Tatsumi, Angew. Chem. Int. Ed. 45 (2006) 3090.
- [21] M. Choi, H.S. Cho, R. Srivastava, C. Venkatesan, D.-H. Choi, R. Ryoo, Nat. Mater. 5 (2006) 718.
- [22] D.P. Serrano, J. Aguado, J.M. Escola, J.M. Rodriguez, A. Peral, Chem. Mater. 18 (2006) 2462.
- [23] J. Aguado, D.P. Serrano, J.M. Escola, A. Peral, J. Anal. Appl. Pyrolysis 85 (2009) 352.
- [24] R.A. García, D.P. Serrano, G. Vicente, D. Otero, M. Linares, Stud. Surf. Sci. Catal. 174A (2008) 1091.
- [25] A. Carrero, G. Vicente, R. Rodríguez, M. Linares, G.L. del Peso, Catal. Today 168 (2011) 148.
- [26] R.A. Sheldon, H. vanBekum, Fine Chemical Through Heterogeneous Catalysis, Wiley-VCH, Weinheim, 2000.
- [27] D.P. Serrano, R.A. García, G. Vicente, M. Linares, D. Procházková, J. Cejka, J. Catal. 279 (2011) 366.
- [28] R. van Grieken, J.L. Sotelo, J.M. Menéndez, J.A. Melero, Micropor. Mesopor. Mater. 39 (2000) 135.
- [29] M. Thommes, Powder Technol. Note 31, Quantachrome Instruments, 2002, PN 59000-31.
- [30] B. Gil, S.I. Zones, S.J. Hwang, M. Bejblova, J. Cejka, Phys. Chem. C 112 (2008) 2997.
- [31] D.P. Serrano, R. van Grieken, J.A. Melero, A. García, Appl. Catal., A 269 (2004) 137.
- [32] E. Oldfield, J. Haase, K.D. Schmitt, S.E. Schramm, Zeolites 14 (1994) 101.
- [33] B. Gil, L. Mokrzycki, B. Sulikowski, Z. Olejniczak, S. Walas, Catal. Today 52 (2010) 24.
- [34] K. Góra-Marek, M. Derewinski, P. Sarv, J. Datka, Catal. Today 101 (2005) 131.
- [35] A. Corma, V. Fornés, J.M. Guil, S. Pergher, Th.L.M. Maesencand, J.G. Buglass, Micropor. Mesopor. Mater. 38 (2000) 301.
- [36] Bevilacqua, D. Meloni, F. Sini, R. Monaci, T. Montanari, G. Busca, J. Phys. Chem. C 112 (2008) 9023.
- [37] G. Sartoriand, R. Maggi, Chem. Rev. 101 (2011) 181.
- [38] F. Bigi, S. Carloni, C. Flego, R. Maggi, A. Mazzacani, M. Rastelli, G. Sartori, J. Mol. Catal. A: Chem. 178 (2002) 139.
- [39] D.P. Serrano, R. García, D. Otero, Appl. Catal. A: Gen. 359 (2009) 69.
- [40] M. Bejblova, D. Procházková, J. Cejka, ChemSusChem 2 (2009) 486.
- [41] M. Selvaraj, K. Lee, K.S. Yoo, T.G. Lee, Micropor. Mesopor. Mater. 81 (2005) 343.
- [42] E. Fromentin, J.-M. Coustard, M. Guisnet, J. Catal. 190 (2000) 433.27.
- [43] S.D. Kim, K.H. Lee, J.S. Lee, Y.G. Kirn, K.E. Yoon, J. Mol. Catal. A: Chem. 152 (2000) 33.
- [44] D. Brunel, M. Chamoumi, P. Geneste, P. Moreau, J. Mol. Catal. A 79 (1993) 297.
- [45] C. Meyer, W. Laufer, W.F. Hölderich, Catal. Lett. 53 (1998) 131.
- [46] G.D. Yadav, D.V. Satoskar, J. Chem. Technol. Biotechnol. 69 (1997) 438.
- [47] W.F. Hölderich, J. Röseler, G. Heitmann, A.T. Liebens, Catal. Today 37 (1997) 353.
- [48] R. van Grieken, D.P. Serrano, J.A. Melero, A. García, J. Mol. Catal. A: Chem. 222 (2004) 167.
- [49] R. van Grieken, D.P. Serrano, J.A. Melero, A. García, J. Catal. 236 (2005) 122.
- [50] R.D. Bach, R.C. Klix, Tetrahedron Lett. 26 (1985) 985.
- [51] J.A. Elings, H.E.B. Lempers, R.A. Sheldon, Stud. Surf. Sci. Catal. 105 (1997) 1165.